



# **iJRASET**

International Journal For Research in  
Applied Science and Engineering Technology



---

# **INTERNATIONAL JOURNAL FOR RESEARCH**

IN APPLIED SCIENCE & ENGINEERING TECHNOLOGY

---

**Volume: 4      Issue: VIII      Month of publication: August 2016**

**DOI:**

**[www.ijraset.com](http://www.ijraset.com)**

**Call: ☎ 08813907089**

**E-mail ID: [ijraset@gmail.com](mailto:ijraset@gmail.com)**

# **Modular Cascaded H-Bridge Multilevel PV Inverter by Using Fuzzy Logic Controller with Distributed MPPT for Grid-Connected Applications**

P.Geetharjuna (M.Tech)<sup>1</sup>, M.C.V Suresh (Asst .Professor)<sup>2</sup>

Dept of EEE, Sri Venkateswara College of Engineering, Karakambadi Road, Tirupati, India.

**Abstract:** *This paper presents a modular cascaded H-bridge multilevel photovoltaic (PV) inverter for single- or three-phase grid-connected applications. The modular cascaded multilevel topology helps to improve the efficiency and flexibility of PV systems. To realize better utilization of PV modules and maximize the solar energy extraction, a distributed maximum power point tracking control scheme is applied to both single- and three-phase multilevel inverters, which allows independent control of each dc-link voltage. For three-phase grid-connected applications, PV mismatches may introduce unbalanced supplied power, leading to unbalanced grid current. To solve this issue, a control scheme with modulation compensation is also proposed. An experimental three-phase seven-level cascaded H-bridge inverter has been built utilizing nine H-bridge modules (three modules per phase). Each H-bridge module is connected to a 185-W solar panel. Simulation and experimental results are presented to verify the feasibility of the proposed approach.*

**Index Terms**—*Cascaded multilevel inverter, distributed maximum power point (MPP) tracking (MPPT), modular, modulation compensation, photovoltaic (PV).*

## **I. INTRODUCTION**

### **A. Introduction**

Because of the lack of fossil fuels and ecological issues brought about by ordinary force era, renewable vitality, especially sun powered vitality, has turned out to be exceptionally prevalent. Sun oriented electric-vitality request has become reliably by 20%–25% for every annum in the course of recent years, and the development is generally in framework associated applications. With the remarkable business sector development in framework associated photovoltaic (PV) frameworks, there are expanding interests in network associated PV designs. Five inverter families can be characterized, which are identified with various setups of the PV framework: 1) focal inverters; 2) string inverters; 3) multistring inverters; 4) air conditioning module inverters; and 5) full inverters. Lattice associated PV frameworks are a mainstream and settled innovation because of their commitments to clean vitality era. The point of this innovation is to remove the greatest conceivable vitality out of PV modules by following its MPP, infusing an astounding current into the matrix and upgrading the general effectiveness of the PV framework. The generally high cost of PV modules has driven specialists to concentrate on shabby and imaginative inverter topologies to make PV power era more appealing. This, thusly, has brought about a high differing qualities of inverter topologies and framework designs. Nonetheless, the most widely recognized topology for single-stage matrix associated frameworks is the two-level multi-string inverter [1]. In this topology, a few dc-dc converters, each of which is associated with a PV cluster, share a solitary dc-join as a yield. This topology offers a few preferences, for example, simple extension of the framework power by including more dc-dc converters and PV modules, free MPP following for each PV exhibit and straightforward control plans.

In the previous decade, multilevel inverter topologies [2] have been acquainted with PV applications [3]. These topologies can infuse an excellent current with a low symphonious mutilation to the network, achieve higher efficiencies with low exchanging recurrence methods and wipe out the cumbersome line-side channel and transformer that are required in the coordination of PV frameworks to a high voltage matrix. Also, multilevel topologies highlight a few dc-joins which can be utilized to decrease the impacts of module bungs in PV exhibits.

Among the distinctive sorts of multilevel converters, the CHB is the most appealing topology as a result of its measured quality, basic physical design, littler number of parts, and higher unwavering quality [4,5]. Also, the need of disengaged dc sources makes

## International Journal for Research in Applied Science & Engineering Technology (IJRASET)

this topology a perfect possibility for PV applications.

The designs of PV frameworks are appeared in Fig. 1. Fell inverters comprise of a few converters associated in arrangement; along these lines, the high power and/or high voltage from the mix of the numerous modules would support this topology in medium and vast lattice associated PV frameworks there are two sorts of fell inverters. Fig. 1(e) demonstrates a fell dc/dc converter association of PV modules. Each PV module has its own dc/dc converter, and the modules with their related converters are still associated in arrangement to make a high dc voltage, which is given to an improved dc/air conditioning inverter. This methodology consolidates parts of string inverters and air conditioning module inverters and offers the upsides of individual module greatest force point (MPP) following (MPPT), yet it is not so much unreasonable but rather more productive than air conditioning module inverters. Be that as it may, there are two force transformation stages in this design. Another fell inverter is appeared in Fig. 1(f), where each PV board is associated with its own particular dc/air conditioning inverter, and those inverters are then set in arrangement to achieve a high-voltage level. This fell inverter would keep up the advantages of "one converter for every board, for example, better usage per PV module, capacity of blending diverse sources, and excess of the framework. Furthermore, this dc/air conditioning fell inverter evacuates the requirement for the per-string dc transport and the focal dc/air conditioning inverter, which further enhances the general effectiveness. The secluded fell H-span multilevel inverter, which requires a disconnected dc hotspot for every H-extension, is one dc/air conditioning fell inverter topology. The different dc joins in the multilevel inverter make autonomous voltage control conceivable. Thus, individual MPPT control in each PV module can be accomplished, and the vitality collected from PV boards can be expanded. In the mean time, the particularity and minimal effort of

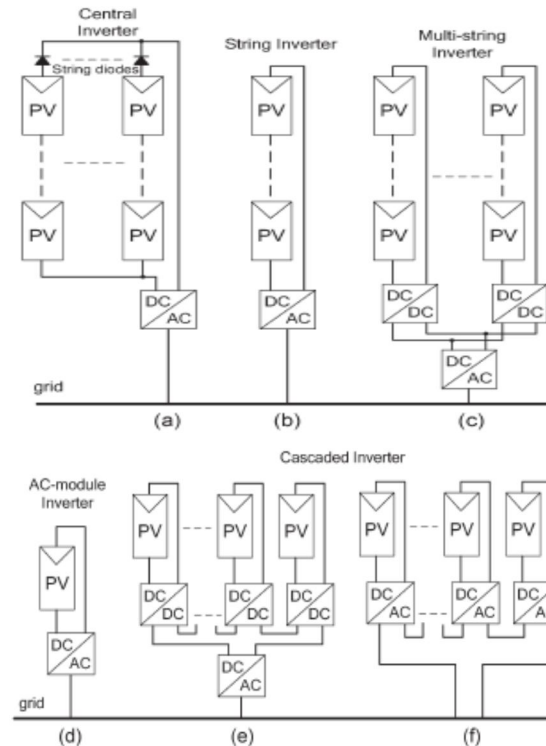


Fig. 1. Configurations of PV systems. (a) Central inverter. (b) String inverter. (c) Multistring inverter. (d) AC-module inverter. (e) Cascaded dc/dc converter. (f) Cascaded dc/ac inverter.

Multilevel converters would position them as a prime possibility for the up and coming era of productive, vigorous, and solid matrix associated sun oriented force gadgets. A secluded fell H-span multilevel inverter topology for single-or three-stage framework associated PV frameworks is exhibited in this paper. The board befuddle issues are tended to demonstrate the need of individual MPPT control, and a control plan with disseminated MPPT control is then proposed. The disseminated MPPT control plan can be connected to both single and three-stage frameworks. What's more, for the exhibited three-stage framework associated PV framework, if each PV module is worked at its own MPP, PV crisscrosses may acquaint uneven force supplied with the three-stage multilevel inverter, prompting lopsided infused lattice current. To adjust the three-stage matrix current, balance pay is likewise

## International Journal for Research in Applied Science & Engineering Technology (IJRASET)

added to the control framework. A three-stage particular fell multilevel inverter model has been manufactured. Every H-extension is associated with a 185-W sunlight based board. The particular outline will expand the adaptability of the framework and lessen the expense too. Reproduction and test results are given to show the created control plan.

### II. CASCADED MULTILEVEL INVERTER

A single-phase structure of an m-level cascaded inverter is illustrated in Figure 31.1. Each separate dc source (SDCS) is connected to a single-phase full-bridge, or H-bridge, inverter. Each inverter level can generate three different voltage outputs,  $+V_{dc}$ , 0, and  $-V_{dc}$  by connecting the dc source to the ac output by different combinations of the four switches,  $S_1$ ,  $S_2$ ,  $S_3$ , and  $S_4$ . To obtain  $+V_{dc}$ , switches  $S_1$  and  $S_4$  are turned on, whereas  $-V_{dc}$  can be obtained by turning on switches  $S_2$  and  $S_3$ . By turning on  $S_1$  and  $S_2$  or  $S_3$  and  $S_4$ , the output voltage is 0. The ac outputs of each of the different full-bridge inverter levels are connected in series such that the synthesized voltage waveform is the sum of the inverter outputs. The number of output phase voltage levels m in a cascade inverter is defined by  $m = 2s + 1$ , where s is the number of separate dc sources. An example phase voltage waveform for an 11-level cascaded H-bridge inverter with 5 SDCSs and 5 full bridges is shown in Figure 31.2. The phase voltage  $v_{an} = v_{a1} + v_{a2} + v_{a3} + v_{a4} + v_{a5}$ . For a stepped waveform such as the one depicted in Figure 31.2 with s steps, the Fourier Transform for this waveform follows.

$$V(\omega t) = 4V_{dc}/\pi \sum_n [\cos(n\theta_1) + \cos(n\theta_2) + \dots \cos(n\theta_s)] \sin(n\omega t)/n, \text{ Where } n=1,3,5,7\dots$$

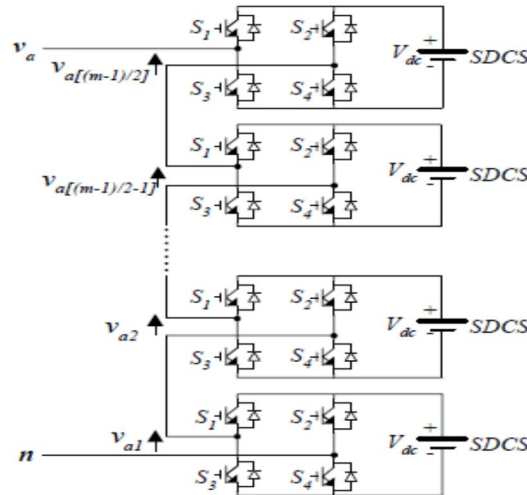


Figure 2. Single-phase structure of a multilevel cascaded H-bridges inverter.

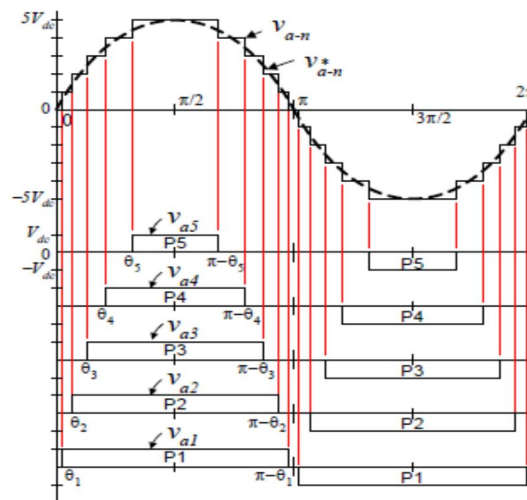


Figure 3. Output phase voltage waveform of an 11-level cascade inverter with 5 separate dc sources.

## International Journal for Research in Applied Science & Engineering Technology (IJRASET)

The Conducting angles  $\theta_1$ ,  $\theta_2$ ,  $\theta_s$ , can be picked such that the voltage all out symphonious twisting is a base. By and large, these edges are picked so that prevalent lower recurrence music, fifth, seventh, eleventh, and thirteenth, music are killed. More detail on consonant end systems will be displayed in the following area.

Multilevel fell inverters have been proposed for such applications as static var era, an interface with renewable vitality sources, and for battery-based applications. Has showed a model multilevel fell static var generator associated in parallel with the electrical framework that could supply or draw responsive current from an electrical framework the inverter could be controlled to either manage the force component of the current drawn from the source or the transport voltage of the electrical framework where the inverter was associated. Have additionally demonstrated that a course inverter can be straightforwardly associated in arrangement with the electrical framework for static var remuneration.

Fell inverters are perfect for interfacing renewable vitality sources with an air conditioner lattice, in light of the requirement for independent dc sources, which is the situation in applications, for example, photograph voltaic or power modules. Fell inverters have likewise been proposed for use as the principle footing drive in electric vehicles, where a few batteries or ultra capacitors are appropriate to serve as SDCs. The fell inverter could likewise serve as a rectifier/charger for the batteries of an electric vehicle while the vehicle was associated with an air conditioner supply. Additionally, the course inverter can go about as a rectifier in a vehicle that utilizes regenerative braking

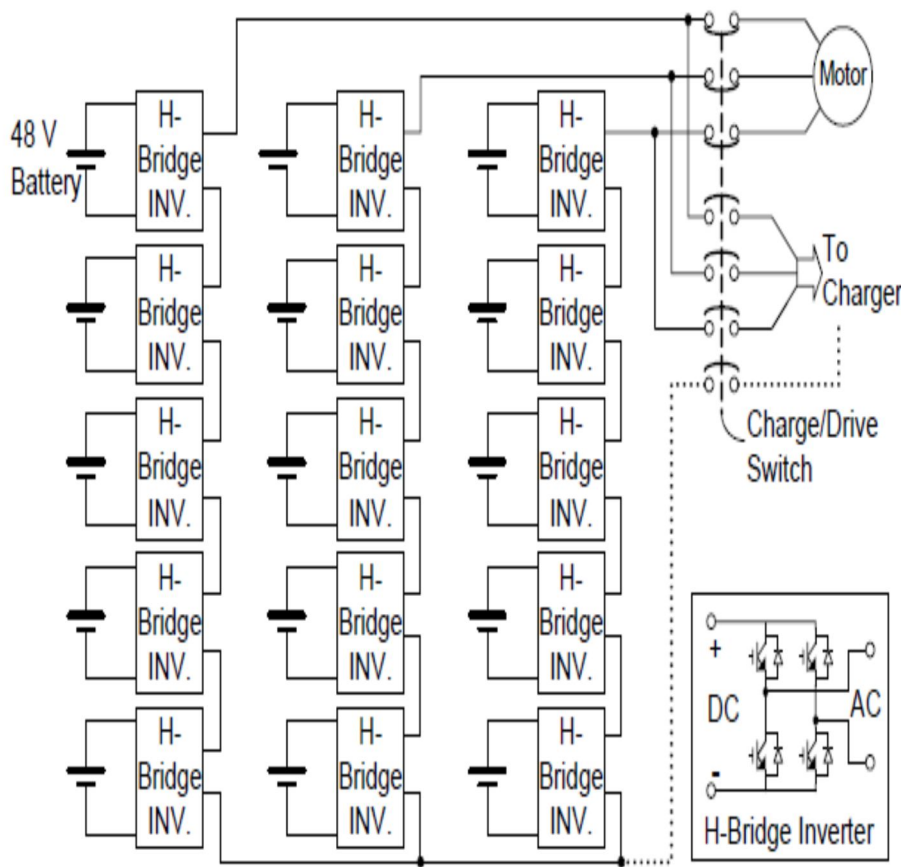


Figure 4. Three-phase wye-connection structure for electric vehicle motor drive and battery charging.

A course topology that uses various dc levels, which as opposed to being indistinguishable in worth are products of each other. He likewise utilizes a mix of major recurrence exchanging for a portion of the levels and PWM exchanging for part of the levels to accomplish the yield voltage waveform. This methodology empowers a more extensive differences of yield voltage extents; nonetheless, it additionally brings about unequal voltage and current evaluations for each of the levels and loses the upside of having the capacity to utilize indistinguishable, secluded units for every level.

# International Journal for Research in Applied Science & Engineering Technology (IJRASET)

## III. SYSTEM DESCRIPTION

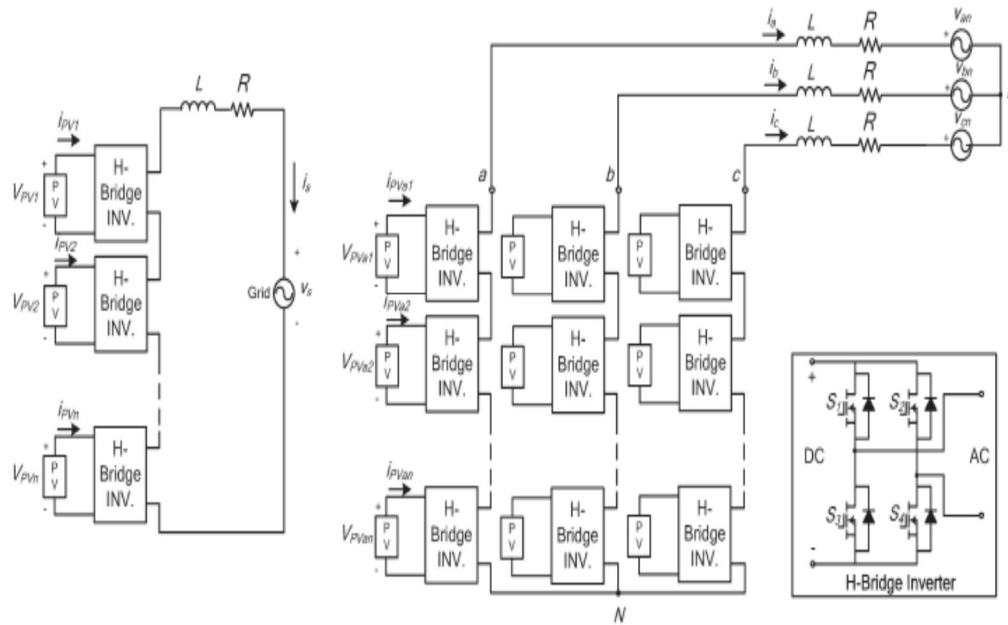


Figure 5. Topology of the modular cascaded H-bridge multilevel inverter for grid-connected PV systems.

Modular cascaded H-bridge multilevel inverters for single and three-phase grid-connected PV systems are shown in Fig. 2. Every stage comprises of  $n$  H-span converters associated in arrangement, and the dc connection of every H-extension can be sustained by a PV board or a short string of PV boards. The full multilevel inverter is associated with the matrix through  $L$  channels, which are utilized to lessen the exchanging music in the current. By various blends of the four switches in every H-span module, three yield voltage levels can be created:  $-v_{dc}$ ,  $0$ , or  $+v_{dc}$ . A full multilevel inverter with  $n$  information sources will give  $2n + 1$  levels to integrate the air conditioner yield waveform. This  $(2n + 1)$ -level voltage waveform empowers the diminishment of music in the blended current, decreasing the extent of the required yield channels. Multilevel inverters additionally have different points of interest, for example, lessened voltage weights on the semiconductor switches and having higher effectiveness when contrasted with other converter topologies.

## IV. PANEL MISMATCHES

PV mismatch is an essential issue in the PV framework. Because of the unequal got irradiance, diverse temperatures, and maturing of the PV boards, the MPP of each PV module might be distinctive. In the event that each PV module is not controlled freely, the effectiveness of the general PV framework will be diminished. To demonstrate the need of individual MPPT control, a five-level two-H-span single-stage inverter is recreated in MATLAB/SIMULINK. Every H-span has its own 185-W PV board associated as a confined dc source. The PV board is demonstrated by detail of the business PV board from Astrometry CHSM-5612M. Consider a working condition that every board has an alternate illumination from the sun; board 1 has irradiance  $S = 1000 \text{ W/m}^2$ , and board 2 has  $S = 600 \text{ W/m}^2$ . In the event that lone board 1 is followed and its MPPT controller decides the normal voltage of the two boards, the force extricated from board 1 would be 133 W, and the force from board 2 would be 70 W, as can be found in Fig. 3. Without individual MPPT control, the aggregate force reaped from the PV framework is 203 W. Be that as it may, Fig. 4 demonstrates the MPPs of the PV boards under the distinctive irradiance. The most extreme yield power qualities will be 185 and 108.5 W when the  $S$  qualities are 1000 and 600  $\text{W/m}^2$ , separately, which implies that the aggregate force collected from the PV framework would be 293.5 W if individual MPPT can be accomplished. This higher worth is around 1.45 times of the one preceding. In this way, individual MPPT control in each PV module is required to build the proficiency of the PV framework. In a three-stage matrix associated PV framework, a PV confuse may bring about more issues. Beside diminishing the general productivity, this could even acquaint unequal force supplied with the three-stage network associated framework. On the off chance that there are PV befuddles between stages, the information force of every stage would be distinctive. Since the network voltage is adjusted, this distinction in information force will bring about lopsided current to the framework, which is not permitted by matrix models. For instance, to

## International Journal for Research in Applied Science & Engineering Technology (IJRASET)

unbalance the current per stage more than 10% is not took into account a few utilities, where the rate lopsidedness is ascertained by taking the greatest deviation from the normal current and isolating it by the normal current

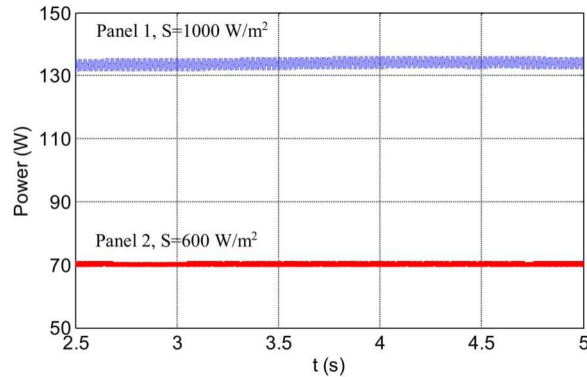


Figure 6. Power extracted from two PV panels.

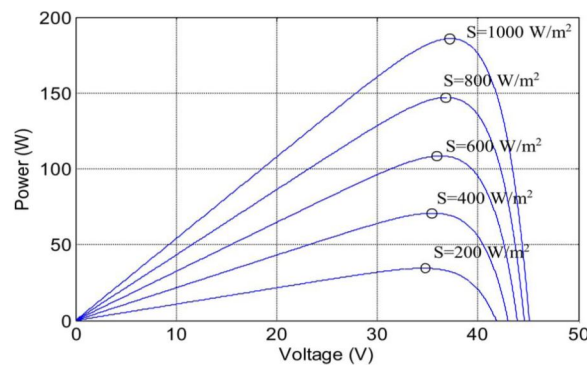


Figure 7.  $P$ - $V$  characteristic under the different irradiance.

To solve the PV mismatch issue, a control scheme with individual MPPT control and modulation compensation is proposed. The details of the control scheme will be discussed in the next section.

### A. Distributed MPPT Control

Keeping in mind the end goal to dispense with the antagonistic impact of the confounds and expand the effectiveness of the PV framework, the PV modules need to work at various voltages to enhance the use per PV module. The different dc joins in the fell H-span multilevel inverter make autonomous voltage control conceivable. To acknowledge individual MPPT control in each PV module, the control plan proposed is upgraded for this application. The conveyed MPPT control of the three-stage fell H-span inverter is appeared in Fig. 5. In every H-span module, a MPPT controller is added to create the dc-join voltage reference. Every dc-join voltage is contrasted with the comparing voltage reference, and the entirety of all mistakes is controlled through an aggregate voltage controller that decides the present reference  $I_{dref}$ . The receptive current reference  $I_{qref}$  can be set to zero, or if responsive force pay is required,  $I_{qref}$  can likewise be given by a responsive current number cruncher. The synchronous reference outline stage bolted circle (PLL) has been utilized to discover the stage point of the matrix voltage. As the great control plan in three-stage frameworks, the matrix streams in abc directions are changed over to dq arranges and managed through proportional-integral (PI) controllers to create the tweak list in the dq organizes, which is then changed over back to three stages.

The appropriated MPPT control plan for the single-stage framework is about the same. The aggregate voltage controller gives the size of the dynamic current reference, and a PLL gives the recurrence and stage point of the dynamic current reference. The present circle then gives the tweak record. To make each PV module work at its own particular MPP, take stage a for instance; the voltages  $vd_{ca2}$  to  $vd_{can}$  are controlled exclusively through  $n - 1$  circles. Every voltage controller gives the regulation list extent of one H-span module in stage a. After increased by the regulation record of stage a,  $n - 1$  balance lists can be acquired. Likewise, the balance list for the primary H-scaffold can be acquired by subtraction. The control plans in stage's b and c are just about the same. The main distinction is that all dc-join voltages are directed through PI controllers, and  $n$  tweak record extents are gotten for every stage.

A phase-shifted sinusoidal pulse width modulation switching scheme is then applied to control the switching devices of each H-bridge. It can be seen that there is one H-bridge module out of  $N$  modules whose modulation index is obtained by subtraction. For single-phase systems,  $N = n$ , and for three-phase systems,  $N = 3n$ , where  $n$  is the number of H-bridge modules per phase. The reason is that  $N$  voltage loops are necessary to manage different voltage levels on  $N$  H-bridges, and one is the total voltage loop, which gives the current reference. So, only  $N - 1$  modulation indices can be determined by the last  $N - 1$  voltage loops, and one modulation index has to be obtained by subtraction. Many MPPT methods have been developed and implemented. The incremental conductance method has been used in this paper. It lends itself well to digital control, which can easily keep track of previous values of voltage and current and make all decisions.

As mentioned earlier, a PV mismatch may bring about more issues to a three-stage secluded full H-span multilevel PV inverter. With the individual MPPT control in every H-span module, the information sunlight based force of every stage would be distinctive, which acquaints unequal current with the framework. To tackle the issue, a zero arrangement voltage can be forced upon the stage legs keeping in mind the end goal to influence the present streaming into every stage. In the event that the overhauled inverter yield stage voltage is corresponding to the uneven force, the present will be adjusted.

Complexity of the control system. First, the unbalanced power is weighted by ratio  $r_j$ , which is calculated as

## International Journal for Research in Applied Science & Engineering Technology (IJRASET)

$$r_j = P_{inav} / P_{inj} \quad (1)$$

Where  $P_{inj}$  is the input power of phase  $j$  ( $j = a, b, c$ ), and  $P_{inav}$  is the average input power. Then, the injected zero sequence modulation index can be generated as

$$d_o = 1/2[\min(r_a \cdot d_a + r_b \cdot d_b + r_c \cdot d_c) + \max(r_a \cdot d_a + r_b \cdot d_b + r_c \cdot d_c)] \quad (2)$$

Where  $d_j$  is the modulation index of phase  $j$  ( $j = a, b, c$ ) and is determined by the current loop controller.

The modulation index of each phase is updated by

$$d'_j = d_j - d_o \quad (3)$$

Only simple calculations are needed in the scheme, which will not increase the complexity of the control system. An example is presented to show the modulation compensation scheme more clearly. Assume that the input power of each phase is unequal

$$P_{ina} = 0.8, P_{inb} = 1, P_{inc} = 1 \quad (4)$$

By injecting a zero sequence modulation index at  $t = 1$  s, the balanced modulation index will be updated, as shown in Fig. 7. It can be seen that, with the compensation, the updated modulation index is unbalanced proportional to the power, which means that the output voltage ( $v_{jN}$ ) of the three-phase inverter is unbalanced, but this produces the desired balanced grid current.

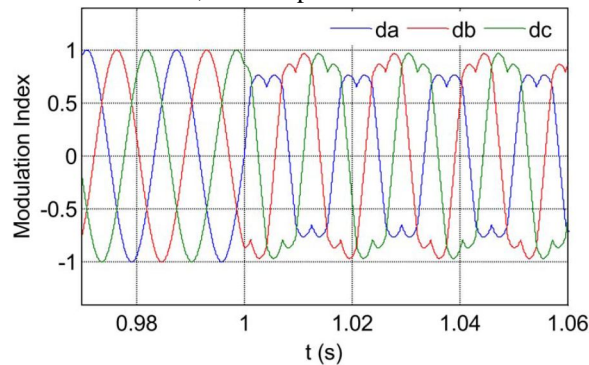


Figure 7. Modulation indices before and after modulation compensation.

TABLE I  
SYSTEM PARAMETERS

Parameters	Value
DC-link capacitor	3600 $\mu$ F
Connection inductor $L$	2.5 mH
Grid resistor $R$	0.1 ohm
Grid rated phase voltage	60 Vrms
Switching frequency	1.5 kHz

### V. SIMULATION RESULTS

Simulation are carried out to validate the proposed ideas.

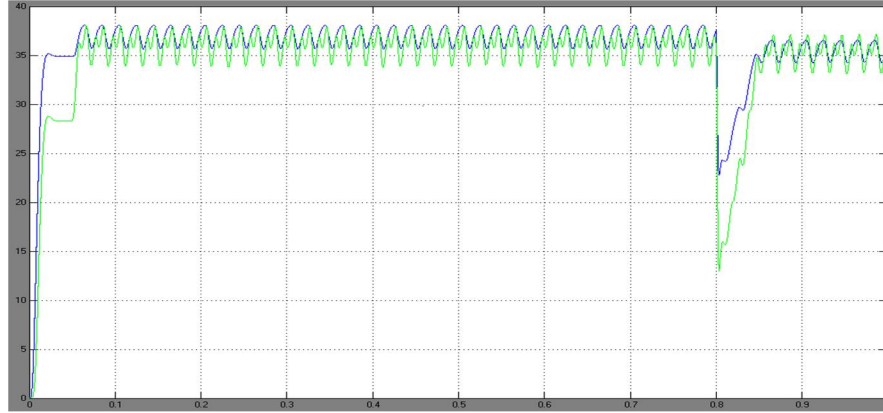
A three-stage seven-level full H-span inverter is recreated and tried. Every H-span has its own 185-W PV board (Astronergy CHSM-5612M) associated as an autonomous source. The inverter is associated with the framework through a transformer, and the stage voltage of the optional side is 60 Vrms. The framework parameters are appeared in Table I.

## International Journal for Research in Applied Science & Engineering Technology (IJRASET)

### A. Simulation Results

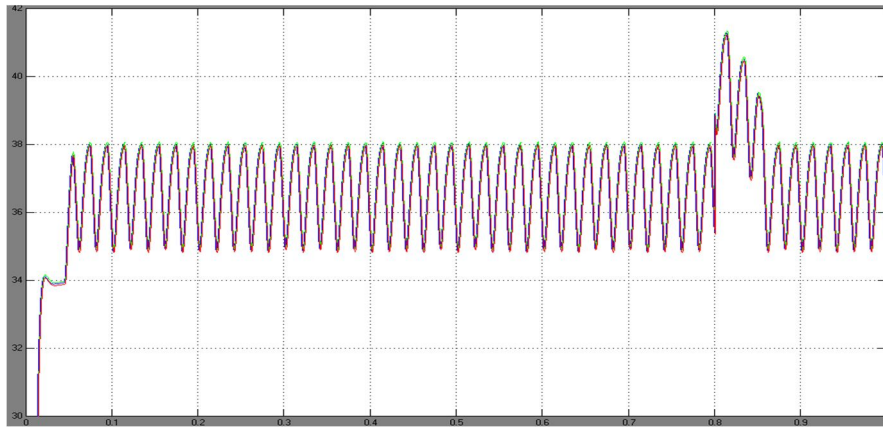
To verify the proposed control scheme, the three-phase gridconnected PV inverter is simulated in two different conditions. First, all PV panels are operated under the same irradiance  $S = 1000 \text{ W/m}^2$  and temperature  $T = 25^\circ\text{C}$ . At  $t = 0.8 \text{ s}$ , the solar irradiance on the first and second panels of phase  $a$

decreases to  $600 \text{ W/m}^2$ , and that for the other panels stays the same. The dc-link voltages of phase  $a$  are shown in Fig. 8. At the beginning, all PV panels are operated at an MPP voltage of  $36.4 \text{ V}$ . As the irradiance changes, the first and second dc-



X-axis: t(s), Y-Axis: V(dc).

(a)

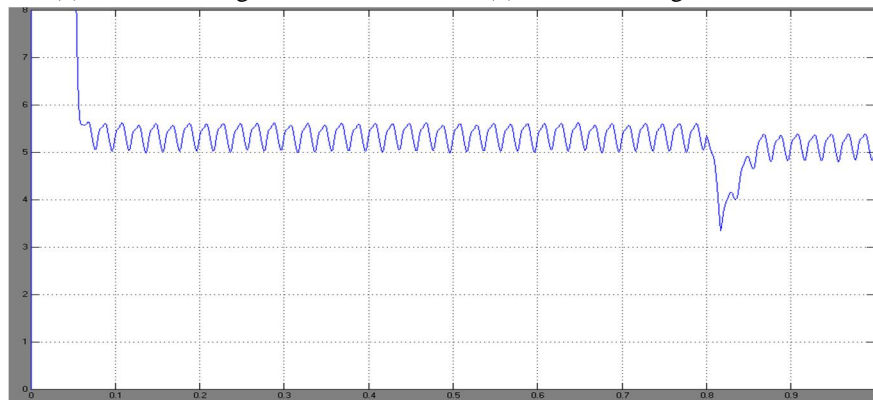


X-axis: t(s), Y-Axis: V(dc).

(b)

Figure. 8. DC-link voltages of phase  $a$  with distributed MPPT ( $T = 25^\circ\text{C}$ ).

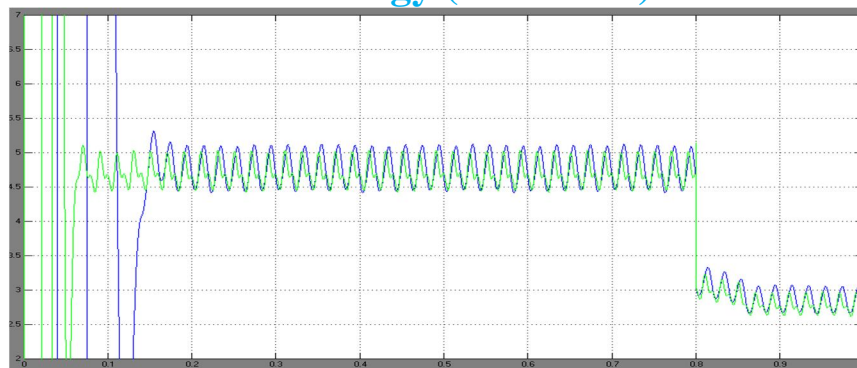
(a) DC-link voltage of modules 1 and 2. (b) DC-link voltage of module 3.



X-axis: t(s), Y-Axis: I(PV).

Figure 9. PV currents of phase  $a$  with distributed MPPT ( $T = 25^\circ\text{C}$ ).

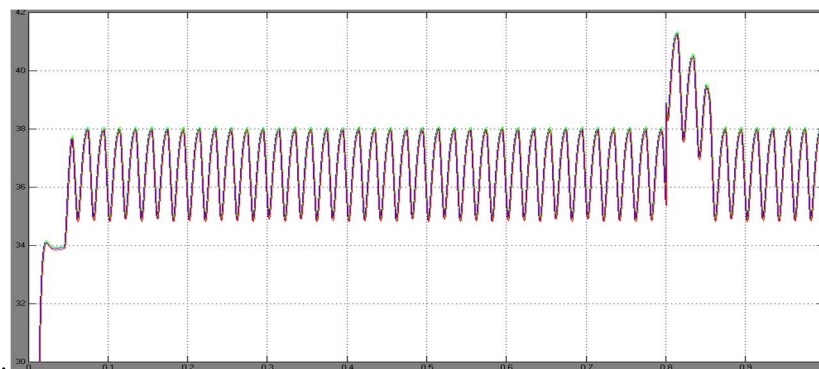
## International Journal for Research in Applied Science & Engineering Technology (IJRASET)



X-axis: t(s), Y-Axis: I(PV).

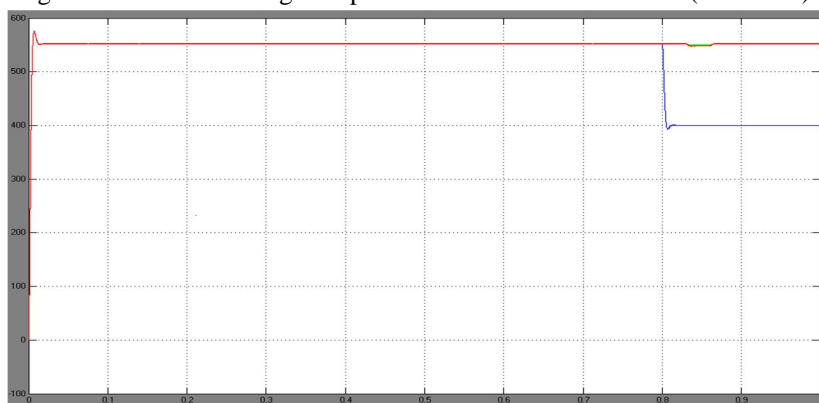
Figure 10. PV currents of phase *a* with distributed MPPT ( $T = 25^\circ\text{C}$ ).

join voltages abatement and track the new MPP voltage of 36 V, while the third board is still worked at 36.4 V. The PV current waveforms of stage an are appeared in Fig. 9. After  $t = 0.8$  s, the streams of the first and second PV boards are much littler because of the low irradiance, and the lower swell of the dc-join voltage can be found in Fig. 8(a). The dc-join voltages of stage b are appeared in Fig. 10. All stage b boards track the MPP voltage of 36.4 V, which demonstrates that they are not impacted by other phases. With the circulated MPPT control, the dc-join voltage of every H-scaffold can be controlled freely. As such, the associated PV board of every H-extension can be worked at its own MPP voltage and won't be impacted by the boards associated with other H-spans. Subsequently, more sunlight based vitality can be removed, and the proficiency of the general PV framework will be expanded



X-axis: t(s), Y-Axis: V(dc).

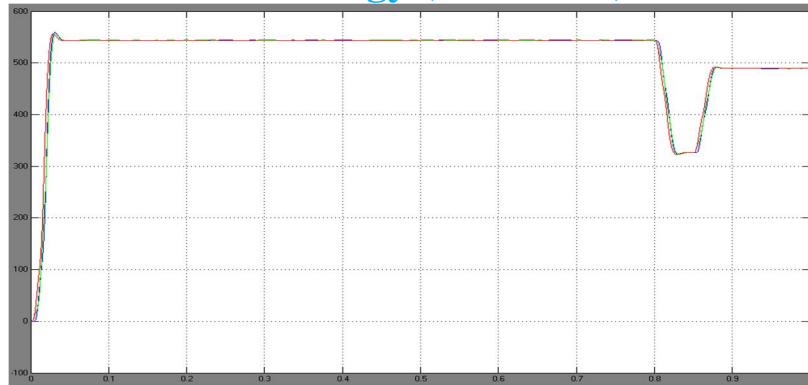
Figure 10. DC-link voltages of phase *b* with distributed MPPT ( $T = 25^\circ\text{C}$ ).



X-axis: t(s), Y-Axis: Power (Wts).

Figure 11. Power extracted from PV panels with distributed MPPT.

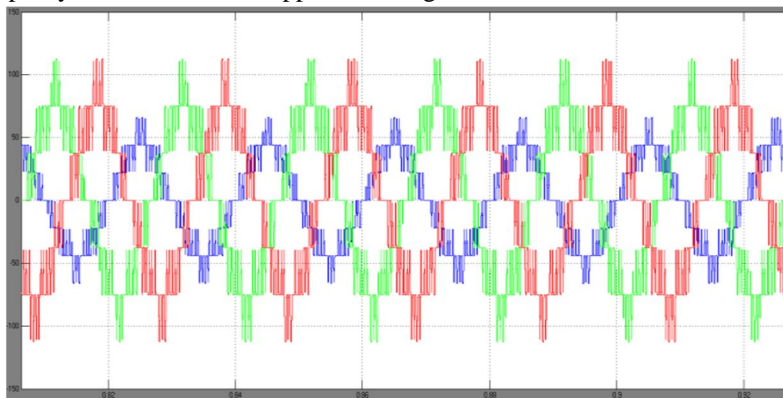
## International Journal for Research in Applied Science & Engineering Technology (IJRASET)



X-axis: t(s), Y-Axis: Power (Wts).

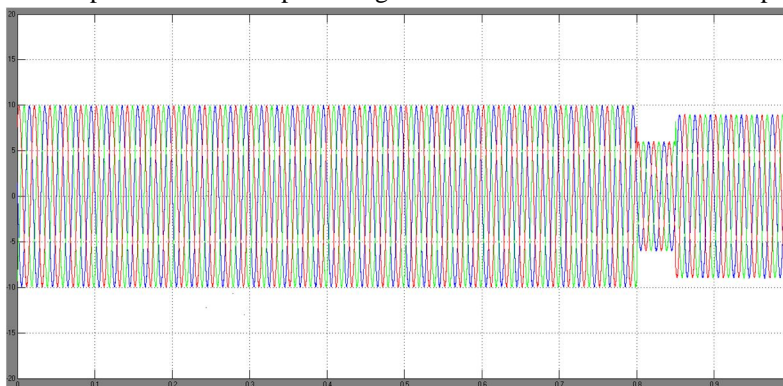
Fig. 12. Power injected to the grid with modulation compensation.

$S = 1000 \text{ W/m}^2$ , and each stage is producing a greatest force of 555 W. After  $t = 0.8 \text{ s}$ , the force gathered from stage a declines to 400 W, and those from the other two stages continue through to the end. Clearly, the force supplied to the three-stage lattice associated inverter is lopsided. Be that as it may, by applying the tweak pay conspire, the force infused to the framework is still adjusted, as appeared in Fig. 12. Likewise, by contrasting the aggregate force separated from the PV boards with the aggregate force infused to the network, it can be seen that there is no additional force misfortune brought on by the adjustment remuneration plan. Fig. 13 demonstrates the yield voltages (vjN) of the three-stage inverter. Due to the infused zero grouping segment, they are lopsided after  $t = 0.8 \text{ s}$ , which parity the lattice current appeared in Fig. 14.



X-axis: t(s), Y-Axis: Voltage (V).

Fig. 13. Three-phase inverter output voltage waveforms with modulation compensation.



X-axis: t(s), Y-Axis: Current (A).

Figure 14. Three-phase grid current waveforms with modulation compensation.

# International Journal for Research in Applied Science & Engineering Technology (IJRASET)

## VI. CONCLUSION

In this paper, a measured full H-span multilevel inverter for network associated PV applications has been displayed. The multilevel inverter topology will enhance the usage of associated PV modules if the voltages of the different dc connections are controlled freely. In this way, an appropriated MPPT control plan for both single and three-stage PV frameworks has been connected to expand the general productivity of PV frameworks. For the three-stage framework associated PV framework, PV befuddles may present unequal supplied power, bringing about uneven infused network current. A tweak pay plan, which won't expand the many-sided quality of the control framework or cause additional force misfortune, is added to adjust the lattice current.

A secluded three-stage seven-level full H-span inverter has been implicit the research center and tried with PV boards under various halfway shading conditions. With the proposed control conspire, each PV module can be worked at its own particular MPP to boost the sunlight based vitality extraction, and the three-stage framework current is adjusted even with the unequal supplied sun based force.

## REFERENCES

- [1] J. M. Carrasco et al., "Power-electronic systems for the grid integration of renewable energy sources: A survey," IEEE Trans. Ind. Electron., vol. 53, no. 4, pp. 1002–1016, Jun. 2006.
- [2] S. B. Kjaer, J. K. Pedersen, and F. Blaabjerg, "A review of single-phase grid connected inverters for photovoltaic modules," IEEE Trans. Ind. Appl., vol. 41, no. 5, pp. 1292–1306, Sep./Oct. 2005.
- [3] M. Meinhardt and G. Cramer, "Past, present and future of grid connected photovoltaic- and hybrid power-systems," in Proc. IEEE PES Summer Meet., 2000, vol. 2, pp. 1283–1288.
- [4] M. Calais, J. Myrzik, T. Spooner, and V. G. Agelidis, "Inverter for single phase grid connected photovoltaic systems—an overview," in Proc. IEEE PESC, 2002, vol. 2, pp. 1995–2000.
- [5] J. M. A. Myrzik and M. Calais, "String and module integrated inverters for single-phase grid connected photovoltaic systems—A review," in Proc. IEEE Bologna Power Tech Conf., 2003, vol. 2, pp. 1–8.
- [6] F. Schimpf and L. Norum, "Grid connected converters for photovoltaic, state of the art, ideas for improvement of transformer less inverters," in Proc. NORPIE, Espoo, Finland, Jun. 2008, pp. 1–6.
- [7] B. Liu, S. Duan, and T. Cai, "Photovoltaic DC-building-module-based BIPV system—Concept and design considerations," IEEE Trans. Power Electron., vol. 26, no. 5, pp. 1418–1429, May 2011.
- [8] L. M. Tolbert and F. Z. Peng, "Multilevel converters as a utility interface for renewable energy systems," in Proc. IEEE Power Eng. Soc. Summer Meet., Seattle, WA, USA, Jul. 2000, pp. 1271–1274.
- [9] H. Ertl, J. Kolar, and F. Zach, "A novel multi cell DC–AC converter for applications in renewable energy systems," IEEE Trans. Ind. Electron., vol. 49, no. 5, pp. 1048–1057, Oct. 2002.
- [10] S. Daher, J. Schmid, and F. L. M. Antunes, "Multilevel inverter topologies for stand-alone PV systems," IEEE Trans. Ind. Electron., vol. 55, no. 7, pp. 2703–2712, Jul. 2008.
- [11] G. R. Walker and P. C. Sernia, "Cascaded DC–DC converter connection of photovoltaic modules," IEEE Trans. Power Electron., vol. 19, no. 4, pp. 1130–1139, Jul. 2004.
- [12] E. Roman, R. Alonso, P. Ibanez, S. Elorduizapaterietxe, and D. Goitia, "Intelligent PV module for grid-connected PV systems," IEEE Trans. Ind. Electron., vol. 53, no. 4, pp. 1066–1073, Jun. 2006.
- [13] F. Filho, Y. Cao, and L. M. Tolbert, "11-level cascaded H-bridge grid tied inverter interface with solar panels," in Proc. IEEE APEC Expo., Feb. 2010, pp. 968–972.
- [14] C. D. Townsend, T. J. Summers, and R. E. Betz, "Control and modulation scheme for a cascaded H-bridge multi-level converter in large scale photovoltaic systems," in Proc. IEEE ECCE, Sep. 2012, pp. 3707–3714.
- [15] B. Xiao, L. Hang, and L. M. Tolbert, "Control of three-phase cascaded voltage source inverter for grid-connected photovoltaic systems," in Proc. IEEE APEC Expo., Mar. 2013, pp. 291–296.
- [16] Y. Zhou, L. Liu, and H. Li, "A high-performance photovoltaic module integrated converter (MIC) based on cascaded quasi-Z-source inverters (qZSI) using eGaN FETs," IEEE Trans. Power Electron., vol. 28, no. 6, pp. 2727–2738, Jun. 2013.
- [17] J. Rodriguez, J. S. Lai, and F. Z. Peng, "Multilevel inverters: A survey of topologies, controls, and applications," IEEE Trans. Ind. Electron., vol. 49, no. 4, pp. 724–738, Aug. 2002.
- [18] Standard for Electric Installation and Use. [Online]. Available: <https://www.xcelenergy.com/>
- [19] A. Dell'Aquila, M. Liserre, V. Monopoli, and P. Rotondo, "Overview of PI-based solutions for the control of DC buses of a single-phase H-bridge multilevel active rectifier," IEEE Trans. Ind. Appl., vol. 44, no. 3, pp. 857–866, May/Jun. 2008.
- [20] B. Xiao, K. Shen, J. Mei, F. Filho, and L. M. Tolbert, "Control of cascaded H-bridge multilevel inverter with individual MPPT for grid-connected photovoltaic generators," in Proc. IEEE ECCE, Sep. 2012, pp. 3715–3721.



10.22214/IJRASET



45.98



IMPACT FACTOR:  
7.129



IMPACT FACTOR:  
7.429



# INTERNATIONAL JOURNAL FOR RESEARCH

IN APPLIED SCIENCE & ENGINEERING TECHNOLOGY

Call : 08813907089  (24\*7 Support on Whatsapp)